14th Australasian Fluid Mechanics Conference
Adelaide University, Adelaide, Australia
10-14 December 2001

An Experimental And Numerical Investigation of Taylor Vortex Flow in The System of Coaxial Rotating Conical Cylinders

M.N. Noui-Mehidi, N. Ohmura and K. Kataoka

Department of Chemical Science and Engineering
Kobe University, Rokkodai, Nada, Kobe 657-8501, JAPAN

Abstract

In the present work both experimental and numerical investigations are combined for the study of Taylor Vortex Flow (TVF) between coaxial conical cylinders with the inner one rotating and the outer one at rest. The numerical simulations are conducted by the use of a finite difference method applied to the SMAC formulation. These simulations permitted the study of the apex angle effect on the development of Taylor vortices. In the steady TVF three modes of six, seven and eight pairs of steady Taylor vortices are observed when the inner conical cylinder rotation is accelerated linearly with different acceleration rates β. The experimental results involve flow visualization and an electrochemical method (polarography) for investigating the time dependency of the flow structures.

Introduction

In recent studies, the effect of the flow structure on the mechanism of transfer in the fluid has been an important subject for many works [6,2]. In the Taylor-Couette flow, since the pioneering work of Taylor [7], geometrical and dynamical effects are still under investigation. Lim *et al.* [3] found new flow regime in a Taylor-Couette flow when the inner cylinder is accelerated very fast. For a better understanding of the geometrical effects on this rotating flow, other hybrid flow systems with constant axial gap width have also been studied as the flow between rotating spheres [8] and between rotating conical cylinders [9,1].

As distinct from the circular Couette flow, a flow between coaxial rotating conical cylinders presents some interesting advantages for some applied processes. Wimmer [9] reported experimentally that different Taylor vortex flow modes between the conical cylinders could be obtained for different dynamical and geometrical arrangements. In this flow system the occurrence of Taylor vortices and the flow properties depend on the apex angle. Hoffman and Busse [1] investigated numerically the instabilities occurring between the cones when the apex angle varies in the limit of the small gap approximation. They found a transition from Taylor vortex instability to Ekman-type instability at a cone angle of about 45 degrees. This result has been experimentally confirmed and discussed by Wimmer [10].

The aim of this investigation was the numerical study of the conical apex angle effect on the occurrence of Taylor vortices when the inner conical cylinder rotation was accelerated linearly and the outer one kept stationary. Experimentally, both visualization and polarography were employed to characterize the different flow structures observed with regard to the different acceleration rates imposed.

Experimental setup

The experimental apparatus in figure 1 consists of an inner conical cylinder of stainless steel and an outer transparent conical cylinder of acrylic resin. The inner one is rotated and the outer one at rest. The maximum radii of the inner and outer conical cylinders are R_{ih}= 42 mm and R_{oh} = 50 mm, respectively, at the top of the flow system, where the radius ratio is η = 0.84 . The two conical bodies have the same half apex angle α = 8 degrees, which makes the gap width constant and equal to d = 8 mm. The height of the working fluid column L = 125 mm gives the aspect ratio Γ = 15.62 . The end plates are fixed to the outer conical cylinder. The outside of the outer conical cylinder is rectangular for flow visualization.

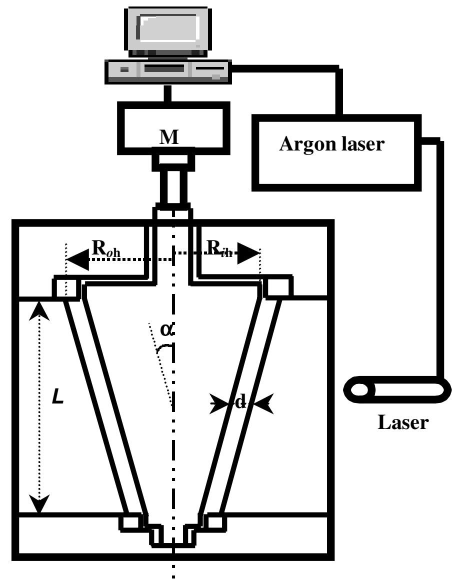

Figure 1. Experimental apparatus

The working fluid was an aqueous solution of 66vol% glycerol and 2 % of Kalliroscope AQ1000 was added for flow visualization. The temperature was measured by a thermo couple of Copper / Constantan with accuracy of 0.1 ℃ . The kinematic viscosity of the solution was 14.82 cS at 25 ℃.

The flow structure visualized with the kalliroscope was observed by the use of a high resolution video camera. Argon laser sheet illumination for observing a cross section of the gap between the conical cylinders and reflected white light illumination for observing the front view of the flow system were employed.

The time-dependent instabilities were also studied by the use of an electrochemical method (polarography). For this purpose, a battery of electrode probes were implemented on the inner wall of the outer fixed conical cylinder. The electrolyte was an aqueous solution of 66 vol% glycerol, ferri-ferro potassium cyanide (10^{-2} mol/ l) with an excess of potassium nitrate (1 mol/ l). The signals collected were treated with a DSP software.

Since the conical radii vary axially, it is rather difficult to define a constant Reynolds number as distinct from a circular cylindrical system. Here, as in the case of concentric rotating

cylinders, the Reynolds number is defined as $Re = \frac{R_{ih}\,\Omega\ d}{\nu}$, where Ω is the angular velocity and ν the kinematic viscosity.
The inner conical cylinder was rotated by DC motor giving stable speed in the range 0 ~ 5000 rpm. A speed reducer of a ratio $\frac{1}{3}$ covered the Reynolds number range 0 ~ 1000 in the actual conditions. The DC motor was controlled by a PC in order to fix the acceleration path for start-up operation. In the present work, only linear accelerations are investigated. The inner conical cylinder is accelerated from rest until its final speed according to the relation: $\Omega(t) = \beta \cdot t$, where β is the acceleration rate and t the time. The acceleration rate can be changed in the range between 0.01 and 1.5 rad / s^2. In order to assure steadiness of the flow states, the observation is done after a duration of steady rotation equivalent to 100 times the acceleration duration from the rest to the final speed.

Experimental results

The basic flow in this system is three-dimensional and depends on the angular velocity Ω of the inner conical cylinder, the gap width d, the apex angle 2α and also the axial position as reported by Wimmer [9]. Noui-Mehidi & Bouabdallah [4] showed in one of their previous works that in the laminar flow, local velocity gradients on the inside wall of the outer conical cylinder decrease with decreasing radii in a concentric rotating conical system by the use of an electrochemical method.

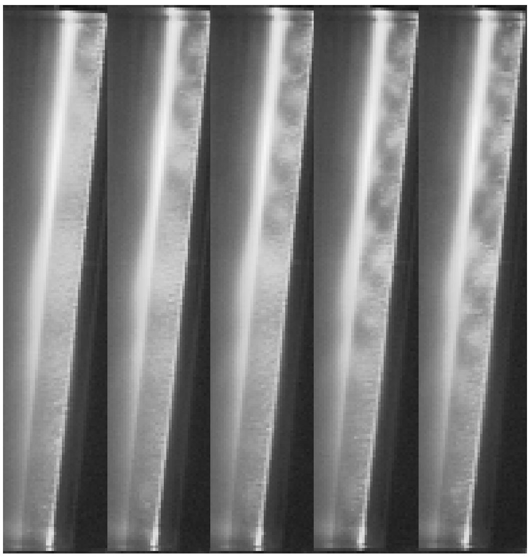

(a) **(b)** **(c)** **(d)** **(e)**

Figure 2. Cross section observation of the first vortices;
(a) Re=138, (b) Re=143, (c) Re=158, (d) Re= 174, (e) Re=182.

When the inner conical cylinder is linearly accelerated from rest, the first transition in the present system occurs at the critical value Re_c = 132. This value represents the first transition boundary common for all the investigated acceleration rates. The first instability occurs due to the birth of a single vortex rotating inward along the upper end plate. In the remaining part of the fluid column, the fluid motion is regulated by the basic meridional circulation directed upward along the rotating wall and downward along the fixed one. When the speed is slowly increased above Re_c, more vortices take place one below the other from the top (figure 2). The neighboring vortices are counter-rotating each other. When three quarters of the fluid column is filled by the vortices, the transition to higher instabilities occurs differently depending on to the acceleration rate of the inner conical cylinder. For acceleration rates varying from 0.01 to 0.07 rad / s^2, i.e. for very low acceleration rates, the first transition is represented by a helical motion taking place in the flow system at the critical value Re_b = 193 from the top. At the value Re_b, if the acceleration rate is in between 0.07 and 1.5, another type of transition occurs. That is, as Re increases from Re_b, with a constant acceleration rate, the first visualized vortices take an upward travelling motion from the bottom to the top. At this state the whole fluid column is filled with vortices. This upward motion diminishes with increasing Re until it stops, and then a train of steady Taylor vortices is obtained. For higher speeds, Taylor vortices become wavy.
The study of the time dependent structures by the use of an electrochemical method (polarography) permitted to follow the evolution of the characteristic frequencies. As stated before for very low acceleration rates, the helical motion occurs with very slow motion for small Reynolds numbers. The ratio of the frequency linked to the helix to the rotational frequency of the inner conical cylinder is found to be 0.36. This ratio remains constant even when the Reynolds number is increased. The power spectrum corresponding to this flow state is presented in figure 3.

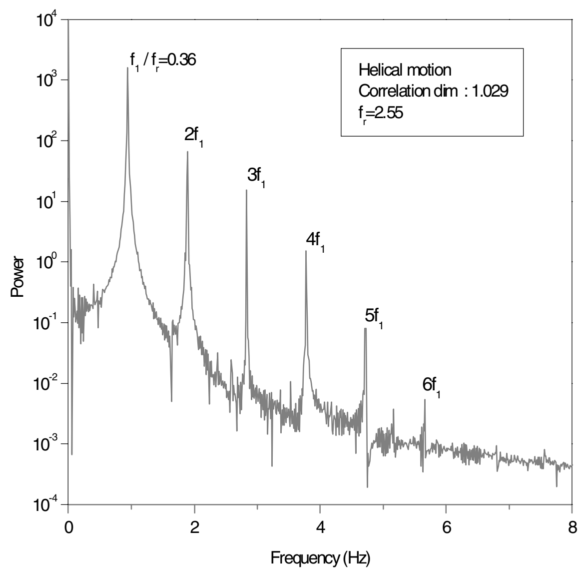

Figure 3. Power spectrum of the helical motion flow state.
(f_1:frequency of the helical motion, f_r:frequency of rotation of inner body).

For moderate acceleration rates of the inner conical cylinder, the upward motion velocity decreases as Reynolds number increases as stated before. The characteristic power spectrum related to this flow state is presented in figure 4.
The decrease of the velocity of this upward motion with regard to Reynolds number can be followed in terms of frequency as shown in figure 5.
When the upward motion stops and according to the acceleration rate of the inner conical cylinder, three modes of steady Taylor vortices can be obtained as presented in figure 6.
In each mode, as observed, the size of the vortices decreases from the bottom to the top of the flow system. This characteristics has also been observed numerically as will be discussed in the next section.

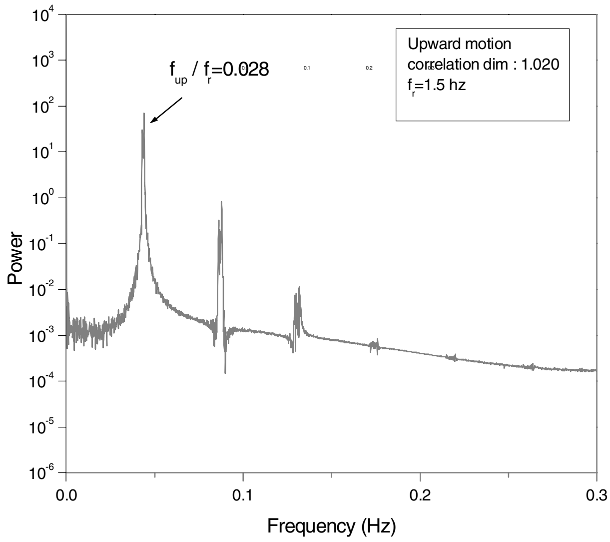

Figure 4. Power spectrum of the upward motion flow state.

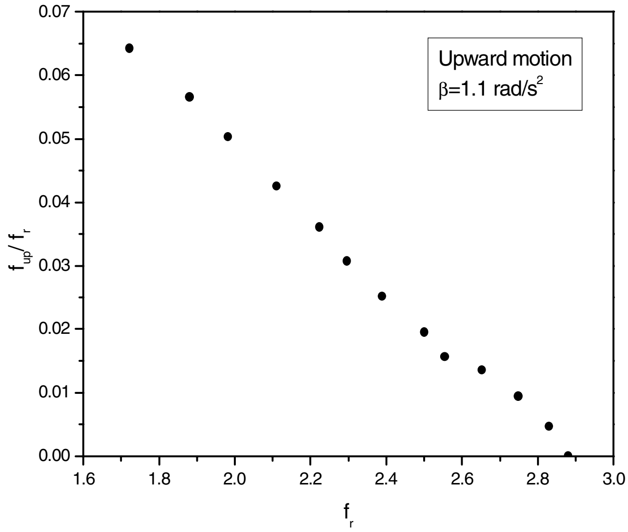

Figure5. Evolution of the ratio of the upward motion frequency to the frequency of rotation of the inner conical cylinder.
(f_{up}:upward motion, f_r: inner conical cylinder rotation frequency)

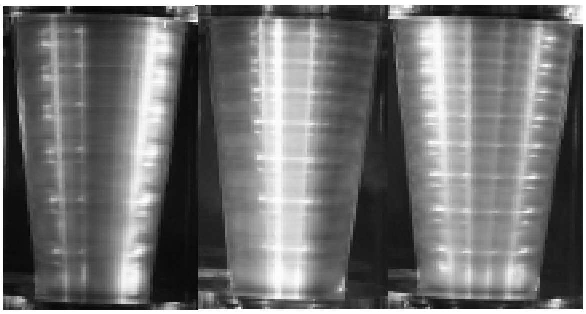

(a) **(b)** **(c)**
Figure 6. Flow visualization of the steady Taylor vortex modes;
(a) six-pair mode, (b) seven-pair mode, (c) eight-pair mode.

When the Reynolds number increases, in each flow mode the steady Taylor vortices become wavy. This wavy motion has the same characteristics as the wavy-vortex flow (WVF) observed in the Couette-Taylor system. In the range of Reynolds number investigated in the present work only single periodic flow has been observed as confirmed by the power spectrum presented in figure 7. As can be seen on figure 7, the frequencies related to the azimuthal waves have in all cases ratios to the frequency of rotation greater than 1.

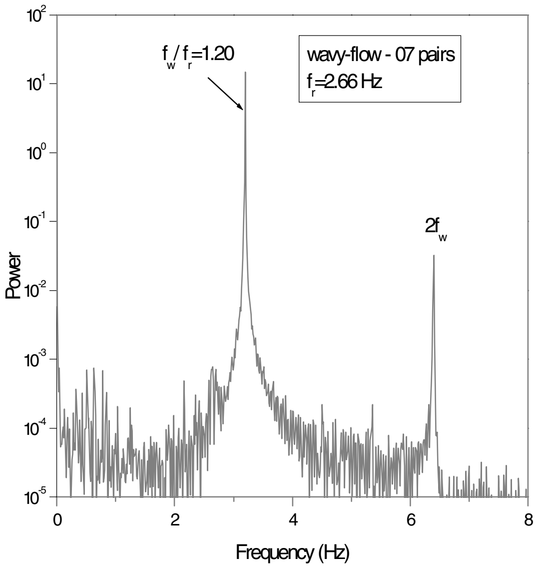

Figure 7. Power spectrum of the seven-pair wavy flow state.
(f_w:frequency of the wavy motion, f_r:frequency of rotation of inner body).

Numerical method

The equations of motion in cylindrical coordinates assuming the axisymmetry of the flow are transformed by the use of a coordinate transformation function which permits to obtain constant boundary conditions on the conical walls. This function is mathematically unique and conformal and given by :

$$\mathbf{f:}\quad \eta = r - z\tan\alpha\;;\quad \xi = z \tag{1}$$

where α is the half conical apex angle.

By applying the coordinates transformation and the corresponding derivatives the equations to be solved are :

$$\frac{Du}{Dt} - \frac{v^2}{\eta+\xi\tan\alpha} = -\frac{\partial P}{\partial \eta} + \frac{1}{Re}\left(\Delta u - \frac{u}{(\eta+\xi\tan\alpha)^2}\right) \tag{2}$$

$$\frac{Dv}{Dt} + \frac{uv}{\eta+\xi\tan\alpha} = \frac{1}{Re}\left(\Delta v - \frac{v}{(\eta+\xi\tan\alpha)^2}\right) \tag{3}$$

$$\frac{Dw}{Dt} = -\frac{\partial P}{\partial \xi} + \tan\alpha.\frac{\partial P}{\partial \eta} + \frac{1}{Re}\Delta w \tag{4}$$

$$\frac{\partial u}{\partial \eta} + \frac{u}{\eta+\xi\tan\alpha} + \frac{\partial w}{\partial \xi} - \tan\alpha.\frac{\partial w}{\partial \eta} = 0 \tag{5}$$

where :

$$\frac{D}{Dt} = \frac{\partial}{\partial t} + \frac{\partial u}{\partial \eta} + \frac{u}{\eta+\xi\tan\alpha} - \tan\alpha.\frac{\partial w}{\partial \eta} + \frac{\partial w}{\partial \xi} \tag{6}$$

$$\Delta = \left(1+\tan^2\alpha\right)\frac{\partial^2}{\partial \eta^2} + \frac{1}{\eta+\xi\tan\alpha}\frac{\partial}{\partial \eta} - 2\tan\alpha.\frac{\partial^2}{\partial\eta\partial\xi} + \frac{\partial^2}{\partial \xi^2} \tag{7}$$

The velocity components are (u,v,w) in the directions given by the cylindrical coordinates (r,θ,z). Putting α=0° in this set of equations leads to the set of equations corresponding to the case of circular rotating cylinders. The numerical approach is done by the use of a first-order time integration scheme with central finite difference method for spacial discretisation. A potential function is applied and Poisson equation is solved with an SOR algorithm according to the SMAC method in order to satisfy the continuity equation. A staggered mesh discretisation is employed. Through numerical experimentation it was confirmed for the case of Γ=9.8 that 11 radial points and 61 axial points were sufficient for the range of Reynolds numbers considered.

Numerical results

After the experimental observation of the Taylor vortices, the study of the apex angle effect on these vortices involving many geometrical situations can be easily achieved numerically.
For the same dynamical and geometrical conditions, varying the apex angle value in the previous system of equations, permits to observe this effect. In the different apex angle configurations numerically simulated, the flow does not develop in the same way between conical cylinders as between circular cylinders as represented in figure 8. For a small aspect ratio Γ=9.8, 10 cells are observed for α=0°,2°,4° and 6°, while only 8 cells exist for α=8°.

In the cylindrical system (α=0°), the cells are symmetric with regard to the mid plane of the fluid column. When α increases, this symmetry is not kept any more and the configurations of the vortices are different depending on α. The conical effect becomes stronger for α=6° and α=8° despite the fact that the number of cells is not the same. As observed by Noui-Mehidi & Wimmer [5], the Taylor vortices in a conical gap are alternately big and small. The big cells are the ones rotating in the direction of the meridional flow and the counter-rotating ones are smaller in size.

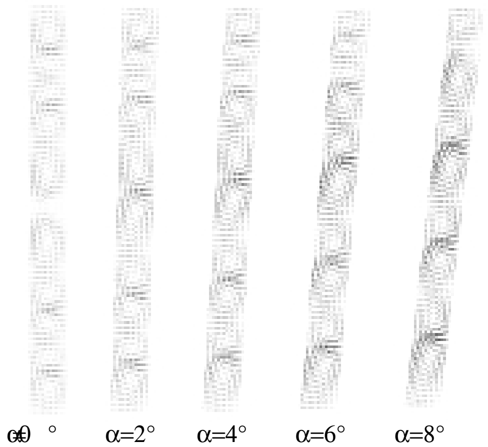

Figure 8. Flow simulations for different values of the apex angle α.

These observations have been confirmed by the present numerical simulation, especially in the case of α=8°.

Following the comparison of the simulations between the different cases of α, the properties of the velocity field, which are practically more difficult to obtain experimentally, are numerically analyzed.

Figure 9 shows the η-distribution of the radial component at the outflow and inflow boundaries. As can be noticed between η=0.5 and 1, u is greater for α=8° than for α=0°, while at η=0.2, for example, u is a little greater for α=0°. This means that the outwards flow becomes slightly faster from the middle of the gap in the conical system. In the inflow boundary region, it can be noticed from figure 9 that in all the gap, the inward motion directed towards the inner rotating wall is much faster for α=0°. The tangential velocity component at the outflow boundary, as can be seen in figure10, at all the radial positions is greater for α=8°.

On the contrary, from figure 10, the inflow boundary seems to behave differently. While v is slightly higher for α=0° in the 2/ 3 of the gap from the outer wall, the tendency is reversed in the neighborhood of the inner wall, where v becomes higher in the case of α=8°. This means that in the inflow boundary region, the fluid is pumped faster by the rotating wall in the conical case.

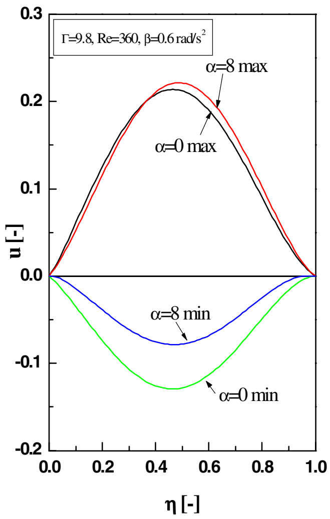

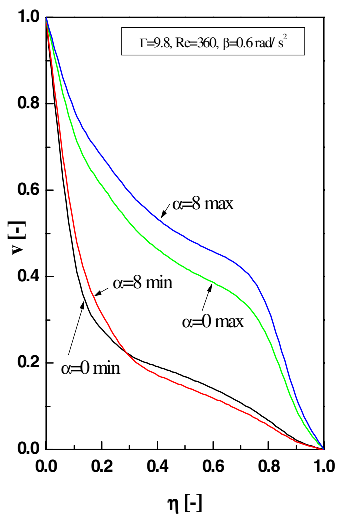

Figure 9. radial evolution of u. Figure10. radial evolution of v.
(max: outflow boundary, min: inflow boundary)

Conclusions

The flow system investigated in the present work presents a rich variety of hydrodynamic instabilities according to the apex angle value and the acceleration rate of the rotation of the inner conical cylinder. The transition from the laminar state is not the same as in the Taylor-Couette flow system since, according to the acceleration rate, there is a bifurcation branching in the present flow system. On the other hand the apex angle seems to affect strongly the disposition and the symmetry of the Taylor vortices observed between the conical cylinders. These properties make of this flow system another typical example of hydrodynamic transition among the other known rotating flow systems.

References

[1] Hoffmann, N.P. & Busse, F.H., Instabilities of Shear Flows between Two Coaxial Differentially rotating cones, *Phy. Fluids*, **11**, 1999,1676-1678.

[2] Khellaf, K., Lauriat, G. & Legrand, J., Numerical Tracking and Circulation Time Distribution in an Infinite Taylor System, *Chem. Eng. Sci.*,**55**, 2000, 767-771.

[3] Lim, T.T., Chew, Y.T. & Xiao, Q., A new Flow Regime in a Taylor-Couette System, *Phys. Fluids*, **10**, 1998, 3233-3235.

[4] Noui-Mehidi, M.N. & Bouabdallah, A. , Laminar-Turbulent Transition between Rotating Cones, *3rd International Workshop "ED Diagnostics of Flows". (Editors: Deslouis, C.; Tribollet, B.) Dourdan (France)* May 9-12, 1993, 139-147.

[5] Noui-Mehidi, M.N. & Wimmer, M. , Free Surface Effects on the Flow between Conical Cylinders, *Acta Mech.* **135**, 1999,13-25.

[6] Ohmura, N., Kataoka, K., Kataoka, T., Shibata, Y. & Makino, T., Effective Mass Diffusion Over Cell Boundaries in a Taylor-Couette Flow System, *Chem. Eng. Sci.*, **52**,N°11,1997, 1757-1765.

[7] Taylor, G.I., Stability of a Viscous Fluid Contained between Rotating Cylinders, *Phil. Trans. R. Soc. London*, **A**, 1923, 223-289.

[8] Wimmer, M., Experiments on a Viscous Fluid Flow between Concentric Rotating Spheres, *J. Fluid Mech.*, **78**, 1976, 317-335.

[9] Wimmer, M., An Experimental Investigation of Taylor Vortex Flow between Conical Cylinders, *J. Fluid Mech.* **292**, 1995, 205-227.

[10] Wimmer, M., Taylor vortices at different geometries, *Physics of Rotating Fluids, Edited by C. Egbers & G. Pfister, Springer, Berlin,*2000, 195-212.